Understanding the Correlation between Ga Speciation and Propane Dehydrogenation Activity on Ga/H-ZSM-5 Catalysts

Yong Yuan¹, Casper Brady¹, Raul F. Lobo¹, Bingjun Xu*,1,2

¹Center for Catalytic Science and Technology, Department of Chemical and Biomolecular Engineering, University of Delaware, Newark, Delaware 19716, United States

²College of Chemistry and Molecular Engineering, Peking University, Beijing 100871, China

Emails: <u>b_xu@pku.edu.cn</u>

Abstract

H-ZSM-5 zeolite supported Ga (Ga/H-ZSM-5) has been considered as a selective catalyst for non-oxidative propane dehydrogenation (PDH) for decades, however, the reaction mechanism remains a topic of considerable discussion. In particular, the correlation between various Ga species present on the catalyst at the reaction conditions and the PDH activity has yet to be established. In this work, intrinsic PDH rates and activation energies were determined on Ga⁺-H⁺ pair sites and isolated Ga⁺ sites for the time on Ga/H-ZSM-5 samples with a wide range of Si/Al and Ga/Al ratios. The turnover frequency on Ga⁺-H⁺ pair sites in the PDH is higher than that of isolated Ga⁺ by a factor of ~15. Experimental measurements combined with a dual-site model show the activation energy in the PDH on the Ga⁺-H⁺ pair sites and isolated Ga⁺ sites to be 90.8 ±1.5 and 117 ± 4.7 kJ·mol⁻¹, respectively. These results demonstrate that Ga⁺-H⁺ pair sites are much more active in the PDH than isolated Ga⁺ sites. Activation energy of GaH_x decomposition to form H₂ was determined to be 40-60 kJ·mol⁻¹ higher than that of the PDH on Ga species, suggesting that the GaH_x decomposition is unlikely to be part of the PDH mechanism. Although both Brønsted acid and Ga sites interact with propane, FTIR results provide strong evidence suggesting that the alkyl mechanism is more likely in the PDH on Ga/H-ZSM-5.

Keywords: propane dehydrogenation, activation energy, Ga^+-H^+ pair sites, isolated Ga^+ sites, alkyl mechanism

Introduction

The increasing demand for propylene and an abundant supply of propane in shale gas has led to a resurgence in the interest in the direct propane dehydrogenation (PDH) reaction. [1-7] Catalysts employed in the two commercial PDH processes, i.e., supported Pt-Sn for the Oleflex process and CrO_x/Al₂O₃ for the Catofin process, suffer from either high cost and fast deactivation or undesirable environmental impact, [1] which incentivizes the search for alternative catalysts. A large number of catalysts have been investigated, including Ga-based, [8-16] V-based, [17-20] Zn-based, [21,22] Co-based, [23-25] Fe-based, [26-28] In-based, [29] Zr-based, [30-32] and nanocarbon catalysts [33,34]. H-ZSM-5 zeolite supported Ga (Ga/H-ZSM-5) has been considered as not only a promising PDH catalyst for its high selectivity, but also an effective catalyst in the propane dehydroaromatization (the Cyclar process). [2]

Despite the extensive literature on Ga/H-ZSM-5, the determination of active spcies and the mechanism in the PDH reaction remain topics of considerable discussion. Earlier studies by Iglesia and coworkers proposed that the Brønsted acid sites (BAS) of H-ZSM-5 activated propane and Ga species acted as portholes to remove H atoms produced in the PDH in the form of H₂ (carbenium mechanism).^[35,36] The applicability of this mechanism was later extended to Zn/H-ZSM-5 and Co/H-ZSM-5.^[37,39] Hensen and coworkers employed diffuse reflectance infrared Fourier Transform spectroscopy (DRIFTS) to demonstrate the replacement of Brønsted acid sites (BAS) by gallium after reduction at high temperature and formation of GaH_x including Ga monohydride (2059 cm⁻¹) and Ga dihydride (2041 cm⁻¹), and suggested that GaH_x may play an important role in PDH.^[40-42] They further proposed exchanged Ga species in the zeolite as the sites that activate alkanes to form the corresponding adsorbed alkyl species (alkyl mechanism) based on the observation of Ga-C₂H₅ and GaH_x.^[43] This theory was supported by later experimental and computational results.^[44,45] Several more recent reports hypothesized that the proximity of BAS and Ga species is a vital factor in determining the PDH activity of Ga

species. Lercher and coworkers^[46] reported that Ga⁺–H⁺ pair sites were more active than isolated Ga⁺ sites and the parent H-ZSM-5. Bell and coworkers^[47] proposed that single [GaH]²⁺ sites were the active centers of the PDH reaction, and the catalyst's reactivity normalized by [GaH]²⁺ sites was independent of the Ga/Al ratio. Several factors contribute to the difficulty in elucidating the PDH mechanism on Ga/H-ZSM-5: 1) The high temperature (≥ 500 °C) at which the PDH reaction takes place makes detection of reaction intermediates challenging, and mechanistic hypotheses are based largely on computational insights. 2) Ga/H-ZSM-5 catalysts with a single Si/Al ratio are typically employed in a given work to draw mechanistic conclusions, which relies on an implicit and largely unsubstantiated assumption that the reaction mechanism and active sites are independent of the Si/Al ratio. Different research groups tend to use samples with different Si/Al ratios, which makes direct comparisons difficult. 3) Catalysts are typically characterized ex-situ, at conditions at which Ga speciation could be significantly different from Ga speciation at PDH conditions. In a recent work, we thoroughly characterized Ga/H-ZSM-5 with varying Si/Al ratios (15, 28 and 39) and Ga/Al ratios (0 – 1.7). with in-situ transmission FTIR spectroscopy. [48] We showed that the density of Ga⁺–H⁺ pair sites could be correlated with GaH_x bands on Ga/H-ZSM-5 reduced at 550 °C, and determined stoichiometric factors in the exchange between Ga⁺ and BAS during the reduction of Ga/H-ZSM-5. These insights pave the way for understanding the correlation between the formation of unique Ga species and their PDH activity.

In this work, we determined the turnover frequencies (TOF) and activation energies of Ga^+-H^+ pair and isolated Ga^+ sites in the PDH on Ga/H-ZSM-5 with varying Si/Al ratios (15, 28 and 39) and Ga/Al ratios (0 – 1.7). Ga^+-H^+ pair sites are more active in the PDH than isolated Ga^+ sites by a factor of ~15, and the activation energy of the PDH on the former is ~26 kJ mol⁻¹ lower than the latter. This is the first rigorous determination of intrinsic PDH activity on these two Ga species.^[47] Activation energies of GaH_x decomposition on these samples were also determined in the absence and presence of C_3H_8 . C_3H_8 is shown to accelerate the decomposition of

GaH_x, suggesting its intimate interaction with the sites capable of forming the hydride species. Activation energy of GaH_x decomposition is 40-60 kJ mol⁻¹ higher than that of the PDH on Ga⁺–H⁺ pair and isolated Ga⁺ sites, suggesting against GaH_x decomposition as part of the PDH mechanism. Further in-situ FTIR results provide evidence supporting the alkyl mechanism.

Experimental Section

Catalyst Preparation and Characterizations

NH₄-ZSM-5 samples (Zeolyst, CBV 3024E CBV 5524G and CBV 8014) was calcined at 550 °C for 8 h in flowing air with a ramp rate of 2 °C min⁻¹ to obtain the H-ZSM-5 with varying Si/Al ratios. The Si/Al ratios of the samples determined by X-ray fluorescence (XRF, Rigaku WDXRF) were 15.4 ± 1.3, 27.5 ± 1.9 and 39.0 ± 2.8. Incipient wetness impregnation with an aqueous solution of gallium(III) nitrate hydrate (Sigma-Aldrich) was used to prepared Ga/H-ZSM-5 samples with varying Si/Al and Ga/Al ratios. Ga/MFI (8 wt% Ga), Ga/SiO₂ (2.2 wt% Ga), Ga/Al₂O₃ (8 wt% Ga) were prepared by the same method with siliceous MFI prepared according to a previous report,^[49] SiO₂ (from Sigma-Aldrich, silica gel davisil, grade 646) and Al₂O₃ (Alfa Aesar), respectively. Ga₂O₃ was obtained by calcining gallium(III) nitrate hydrate at 600 °C in flowing air for 2 h with a ramp rate of 5 °C·min⁻¹. The obtained Ga₂O₃ is dominated by the γ phase, as confirmed by XRD measurement on a Bruker D8 diffractometer with Cu Kα radiation (40 kV, 40 mA). Micropore volumes of the samples (Table S1) were determined by N₂ adsorption at -196 °C and the t-plot method. N₂ adsorption isotherms were collected on a Micromeritics 3Flex system. All samples were degassed for 24 h at 300 °C prior to the adsorption measurements. Surface area of the Ga₂O₃ sample was determined to be 80 m²·g⁻¹ via the BET method. In-situ Fourier Transformed Infrared (FTIR) spectra were collected on an Agilent CARY 660 spectrometer equipped

with an MCT detector. Typical spectra presented are 128 coadded scans per spectrum at a spectral resolution of 2 cm⁻¹. Spectra for kinetic analysis are 32 coadded scans to improve the temporal resolution. Chemicals such as H₂, C₃H₈ and C₃H₆ were introduced into the transmission cell and pressure was controlled via the vacuum manifold. The detailed discussion of the preparation and characterization of these samples are shown in ref ^[48].

Catalytic Performance

Catalytic reactions were performed in a fixed-bed plug flow reactor, which consists of a quartz glass tube (1/4 inch in diameter). The catalyst bed typically contained 3.8 – 15 mg of catalyst with a particle size range of 20-40 mesh. Catalysts were diluted with SiO₂ (Sigma-Aldrich, silica gel davisil, grade 646) with a 1:3 mass ratio. A thermocouple was placed directly above the catalyst bed inside the reactor tube to ensure accurate temperature measurement. The thermocouple has no detectable catalytic activity at the reaction temperature. Prior to the catalytic activity measurements, the catalyst was heated to 550 °C for 30 min with a ramp rate of 10 °C·min⁻¹ in 10 vol.% H₂ with balancing N₂ (20 mL·min⁻¹), followed by purging with N₂ at the same temperature. The reduced sample was then exposed to 5 vol.% C₃H₈ with balancing N₂. The total pressure was maintained at 101.32 kPa. Gas flow rates were adjusted in the range of 20 – 100 mL·min⁻¹ to vary the space times, which was defined as mol_{Al}·s·mol_{C3H8}⁻¹ for Ga/H-ZSM-5 samples and g_{Cat}·s·mol_{C3H8}⁻¹ for Ga supported on different supports. The reactor effluent was periodically sampled by an online gas chromatograph (GC) (Agilent 6890), via a heated gas line, equipped with an HP-PLOT/Q column and flame ionization detector (FID) used for product analysis. FID response factors for CH₄, C₂H₄, C₃H₆, C₃H₈ were calibrated prior to the activity measurements. The conversion of C₃H₈ was determined by Eq. 1, the selectivity and yield of CH₄, C₂H₄, C₃H₆ were obtained by Eqs. 2-3.

Conversion =
$$\left(1 - \frac{F_{C_3H_8, \text{ outlet}}}{F_{C_3H_8, \text{ inlet}}}\right) \times 100\%$$
 (1)

Selectivity =
$$\frac{n_i \times F_{i, \text{ outlet}}}{\sum n_i \times F_{i, \text{ outlet}}} \times 100\%$$
 (2)

Yield =
$$\frac{n_i \times F_{i, \text{ outlet}}}{3 \times F_{C_3 H_8, \text{ inlet}}} \times 100\%$$
 (3)

Carbon balance =
$$\frac{3 \times F_{C_3H_8, \text{ outlet}} + \sum_{i, \text{ outlet}} N_i \times F_{i, \text{ outlet}}}{3 \times F_{C_3H_9, \text{ inlet}}} \times 100\%$$
 (4)

where i represents the hydrocarbon product CH₄, C₂H₄, C₃H₆ in the effluent gas, n_i is the number of carbon atoms of component i, F_i is the molar flow rate. The C₃H₈ conversion was measured at differential conversions (<5.5%). PDH rates were determined by the C₃H₆ yields, and C₃H₈ cracking rates were determined by the CH₄ and C₂H₄ yields. Testing the catalyst under low C₃H₈ conversion limited secondary reactions, which was confirmed by the equimolar formation CH₄ and C₂H₄ derived from cracking reaction when product selectivity was extrapolated to zero space time. PDH and cracking rates over Ga/H-ZSM-5 were normalized to the Al content of the catalyst. Apparent activation energies were determined in the temperature range of 530–570 °C. Deactivation was below 5% after 12 h on stream in all cases. Carbon balance (Eq. 4) in all experiments was higher than 97%.

Results and Discussion

Dependence of PDH Rates on Si/Al and Ga/Al Ratios

PDH rates were measured on reduced Ga/H-ZSM-5 with varying Si/Al ratios (15, 28 and 39) and Ga/Al ratios (0 – 1.7). Numerous studies have reported PDH on Ga/H-ZSM-5 with a variety of Si/Al ratio and Ga/Al ratios, however, the reactivity and kinetics were measured at different conditions and on samples prepared by different methods, making direct comparisons difficult.^[46,47,50-52] In this work, all Ga/H-ZSM-5 samples were prepared via impregnation, followed by calcination. These catalysts have been thoroughly characterized in our

recent report, [48] and their key properties are summarized in Tables S1 and S2 of the Supporting Information. Calcined catalysts were reduced in 10 vol.% H_2 for 30 min at 550 °C prior to the introduction of 5 vol% C_3H_8 (5.07 kPa with balancing N_2).

PDH rates were measured in the kinetic regime, as confirmed by the linear correlation between the propane conversion/product yield (C₃H₆, C₂H₄ and CH₄) and the catalyst loading at 550 °C and 570 °C (Figure S1). [47] Rates and selectivities are determined by extrapolating to zero space time (Figure S2) in order to eliminate the impact of product inhibition and secondary reactions.^[47] Stable conversion and good carbon balances were observed during the first 10 h time on stream (TOS) on all catalysts (Figure S3). The selectivity for C₃H₆ increases with decreasing space time while the selectivity for C₂H₄ decreases on Ga/H-ZSM-5 (Si/Al = 15 and Ga/Al = 0.21), while the selectivity for CH₄ remains constant (Figure S2a). At zero space time, the selectivity towards C₂H₄ is close to twice that of CH₄ (on a per carbon atom basis, Eq. 2), which is consistent with the stoichiometry of C₃H₈ cracking into C₂H₄ and CH₄.^[47,53] PDH rates extrapolated to zero space time on a per Al basis (referred to as TOF_{Al}) over Ga/H-ZSM-5 with various Ga/Al and Si/Al ratios are shown in Figure 1a. Rates are expressed in terms of TOF_{Al} to allow for fair comparison among samples with the same Si/Al ratio, which will be converted to rates normalized to specific Ga species later on in this work. On samples with a Si/Al ratio of 15, as the Ga/Al ratio increases, the TOF_{Al} increases rapidly at low Ga loadings up to the Ga/Al ratio of 0.05 and then grows more slowly as the Ga/Al ratio rises to 0.3 before declining as the Ga/Al ratio increases further (Figure 1a). This trend is in general agreement with the results reported by Bell and coworkers, [47] in which Ga/H-ZSM-5 with a Si/Al of 16.5 were employed. TOF_{Al} peaks at a value of 34.0×10^{-3} mol_{C3H8}·mol_{Al} $^{1}\cdot s^{-1}$ at the Ga/Al ratio of 0.31, which is 16 times higher than that on the parent H-ZSM-5 (2.1 \times 10⁻³ mol_{C3H8}·mol_{A1}⁻¹·s⁻¹). The large difference between the PDH rates on Ga/H-ZSM-5 and H-ZSM-5 indicates that the contribution to the overall PDH activity from the residual BAS in Ga/H-ZSM-5 is minor. A much higher enhancement in the PDH rate (by a factor of ~500) after the introduction of Ga to H-ZSM-5 was reported by Bell and coworkers;^[47] this disparity could be attributed to the differences in the reaction conditions, e.g., the reaction temperature (460 °C vs. 550 °C). A similar 3-segment dependence of the PDH rate on the Ga/Al ratio was observed on samples with a Si/Al ratio of 28 (Figure 1a). TOF_{Al} on Ga/H-ZSM-5 with a Si/Al ratio of 39 increases almost linearly up to a Ga/Al ratio of 0.55, before declining at higher Ga/Al ratios (Figure 1a). The result is consistent with the trend reported by Lercher and coworkers, in which Ga/H-ZSM-5 samples with a Si/Al ratio of 50 were employed.^[46] Importantly, Figure 1 shows that TOF_{Al} depends not only on the Ga/Al ratio, but it is also sensitive to the Si/Al ratio of the zeolite. This implies that a mechanistic interpretation of reactivity on samples with a single Si/Al ratio is unlikely to be complete.

A more quantitative analysis of the impact of Si/Al and Ga/Al ratios of Ga/H-ZSM-5 catalysts on the PDH rates reveals two types of active sites. The low Ga/Al range of Figure 1a is replotted in Figure 1b for further analysis: on samples with a Si/Al ratio of 15, the slope of the TOF_{Al} versus the Ga/Al ratio at Ga/Al ratios below 0.042 is fitted to be 0.597±0.091 mol_{C3H8}·mol_{Ga}-1·s-1 (Figure 1b). This slope represents the TOF of

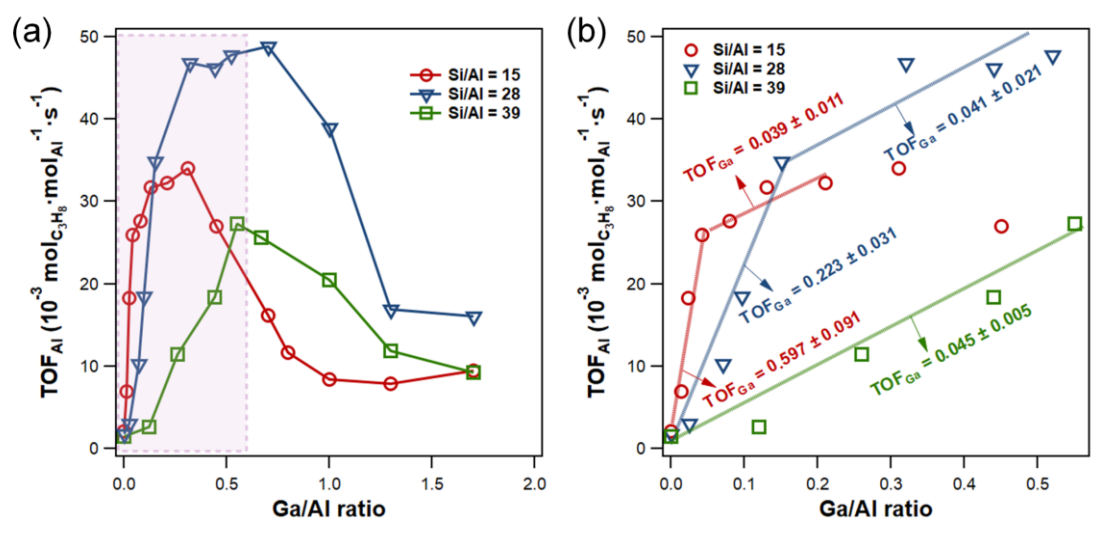


Figure 1. (a) TOF_{Al} as a function of the Ga/Al ratio on H-ZSM-5 with three Si/Al ratios (15, 28, 39), and (b) a zoomed in view of low Ga/Al ratios (boxed region in (a)). Reaction conditions: 550 °C, C₃H₈ partial pressure 5.07 kPa with balancing N₂. The propane conversions are below 5.5% in the rate measurements.

the PDH on a per Ga increment basis, referred to as TOF_{Ga}, which could be viewed as the intrinsic PDH activity of a small amount of Ga added in a given range of Ga/Al ratio. TOF_{Ga} decreases to 0.039±0.011 in the Ga/Al range of 0.042 to 0.21, which is smaller than that in the lower Ga/Al range by a factor of ~15. This drastic change in the TOF_{Ga} implies that additional Ga introduced at in the Ga/Al ratio of 0.042 to 0.21 exists in a different state from that introduced to samples with the lower Ga/Al ratios, i.e., two types of Ga sites with distinct PDH activities are present. Similarly, for samples with a Si/Al ratio of 28, TOF_{Ga} are determined to be 0.223 ± 0.031 and 0.041 ± 0.021 mol_{C3H8}·mol_{Ga}⁻¹·s⁻¹ in the Ga/Al ratio range of 0 – 0.15 and 0.15 – 0.46, respectively. The reduction in the TOF_{Ga} at the higher Ga/Al ratio range (by a factor of ~7) on Ga/H-ZSM-5 (Si/Al = 28) is lower than that on the Al-rich samples (Si/Al = 15). On samples with a Si/Al ratio of 39, TOF_{Ga} is low (0.045±0.005 mol_{C3H8}·mol_{Ga}-1·s-1) from the lowest Ga loading evaluated (Figure 1b). A striking feature of TOF_{Ga} values is that they are similar (0.039 – 0.045 mol_{C3H8}·mol_{Ga}-1·s⁻¹) for Ga/H-ZSM-5 samples with Si/Al ratios of 15 (0.042 \leq Ga/Al \leq 0.21) and 28 (0.15 \leq Ga/Al \leq 0.44) after the initial rapid rise, and the sample with a Si/Al ratio of 39 at Ga/Al ratios below 0.55 (Figure 1b). It can be inferred that within these Ga/Al ratio ranges, increasing the Ga loading introduces the same type of active site in the PDH in all samples. For samples with lower Si/Al ratios (15 and 28), a much more active Ga species is present at very low Ga loadings. Control experiments on unsupported Ga₂O₃, Ga₂O₃ supported on siliceous MFI (Ga/MFI) and Ga₂O₃ supported on Al₂O₃ (Ga/Al₂O₃) show much lower PDH activities compared with H-ZSM-5 and Ga/H-ZSM-5 (Figure S4). This shows that the fraction of Ga₂O₃ in Ga/H-ZSM-5 that does not diffuse into zeolite pores during reduction has a negligible contribution to the PDH rate. Similar trends are observed in the C₃H₈ cracking rates (Figure S5a).^[47] The ratio between the PDH and cracking rates increases monotonically with the Ga/Al ratio on all Ga/H-ZSM-5 samples investigated (Figure S5b), that is, higher amounts of exchanged Ga favors dehydrogenation pathway while BAS promote the cracking of C₃H₈, in agreement with previous literature.^[46]

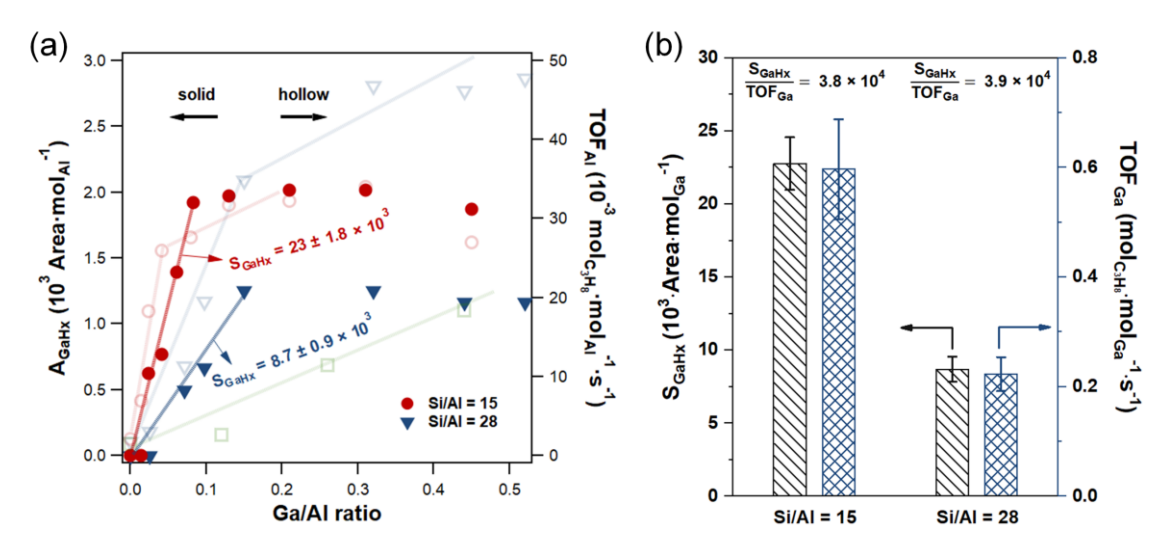


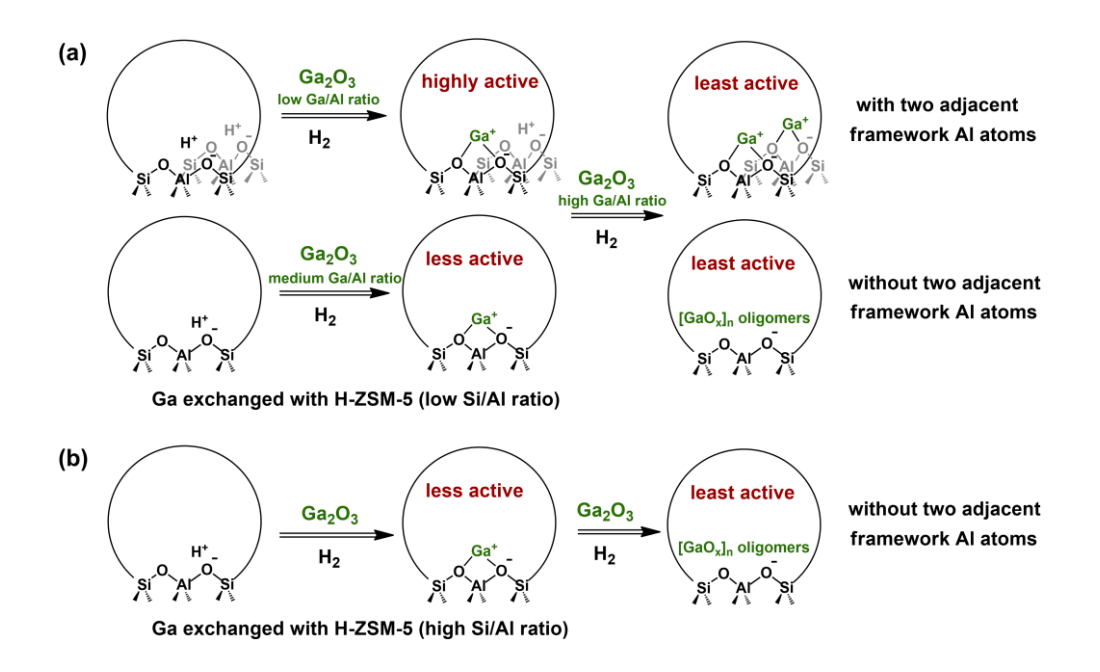
Figure 2. (a) A_{GaHx} (peak area of GaH_x normalized by a per Al basis determined from infrared spectra) as a function of the Ga/Al ratio on H-ZSM-5 with two Si/Al ratios (15 and 28). (b) S_{GaHx} (peak area of GaH_x normalized by a per Ga basis) and TOF_{Ga} (PDH rates normalized by a per Ga basis) between Si/Al ratio of 15 and 28 at low range of Ga/Al ratios. The original data of the spectra showing GaH_x formation as a function of the Ga/Al ratios were discussed in our previous report.⁴⁸ The propane conversions are below 5.5% in the rate measurements.

The observed reactivity trends on Ga/H-ZSM-5 catalysts with different Si/Al and Ga/Al ratios suggest that Ga⁺ – H⁺ pair sites and isolated Ga⁺ sites are the active species in the PDH. Our recent report provided strong evidence for the presence two Ga species, i.e., Ga⁺ – H⁺ pair and isolated Ga⁺ sites, on reduced Ga/H-ZSM-5 with distinct abilities to form GaH_x (a combination of GaH₂ and GaH, with the former being the dominant species) at 550 °C after H₂ treatment. GaH_x species were probed by transmission FTIR spectroscopy, and their abundance was monitored via the integrated area of the corresponding band. The extinction coefficients for these GaH_x species remain unknown, and thus only their relative abundance, at different Ga/Al ratios rather than absolute densities, can be determined. The dependence of GaH_x densities on Si/Al and Ga/Al ratios have been reported in our previous report Hall, which is incorporated in Figure 2a. Importantly, the transition points from rapid to a more gradual rise in the density of the GaH_x species with an increasing Ga/Al ratio in Ga/H-ZSM-5 with Si/Al ratios of both 15 and 28 coincide with those of the TOF_{Ga}, at Ga/Al ratios of 0.074 and 0.15, respectively (Figure 2a). This is a clear indication that the changes in Ga

speciation and the TOF_{Ga} are correlated. The slope of the Al normalized peak area of the GaH_x band (A_{GaHx}) versus the Ga/Al ratio (Figure 2a), referred to as S_{GaHx}, represents the Ga normalized peak area of GaH_x with the unit of $A_{GaHx} \cdot mol_{Ga}^{-1}$. S_{GaHx} on Ga/H-ZSM-5 with Si/Al ratios of 15 and 28 are determined to be $23\pm1.8 \times 10^{-1}$ 10^3 and $8.7\pm0.9\times10^3$ $A_{GaHx}\cdot mol_{Ga}^{-1}$, respectively, at Ga/Al ratios equal to or below 0.1. S_{GaHx}/TOF_{Ga} ratios of Ga/H-ZSM-5 with Si/Al ratios of 15 and 28 agree almost quantitively $(3.8 \times 10^4 \text{ and } 3.9 \times 10^4, \text{ respectively,})$ Figure 2b). This observation further confirms the strong correlation between the Ga species' propensity to form GaH_x and the PDH activity at low Ga/Al ratios (≤ 0.1). In our previous report, we established that the Ga species' ability to form GaH_x after H₂ treatment at 550 °C was dependent on the proximity of Ga⁺ with neighboring BAS, i.e., Ga⁺-H⁺ pair or isolated Ga⁺ sites.^[48] It follows that the relative concentrations of these two types of Ga species are likely responsible for the different dependence of the TOF_{Ga} on the Ga/Al ratio (Figure 1). We have shown that Ga⁺ preferentially exchanges with one H⁺ in proton pairs to form Ga⁺-H⁺ pair sites at low Ga loadings.^[48] Thus, the observed PDH rates on the Ga/H-ZSM-5 catalysts investigated (Figure 1) could be rationalized as follows: On Ga/H-ZSM-5 (Si/Al = 15), only Ga⁺-H⁺ pair sites are initially produced during the reduction of calcined catalyst due to the abundance of paired protons on the Al-rich zeolite at Ga/Al ratios below 0.042; these sites display high PDH rates. In the Ga/Al ratio range of 0.042 – 0.21, only isolated Ga⁺ sites are introduced as the Ga loading increases (Scheme 1a), which is less active in the PDH reaction. Increasing the Ga/Al ratio further beyond 0.21 leads to the replacement of the protons present in Ga⁺-H⁺ pair sites with Ga⁺ to form relatively inactive Ga⁺-Ga⁺ pair sites, leading to a further decrease in the TOF_{Ga}. On Ga/H-ZSM-5 (Si/Al = 28), the lower density of proton pairs—as compared to that on the Al-rich sample—leads to the formation of both Ga^+-H^+ pair sites and isolated Ga^+ sites even at low Ga/Al ratios (0 – 0.15), and thus TOF_{Ga} is lower than that on samples with only Ga⁺–H⁺ pair sites. In the Ga/Al ratio range of 0.15 – 0.52, only isolated Ga⁺ sites are introduced with increasing Ga loading, leading to a similar TOF_{Ga} to that on Ga/H-ZSM-5 (Si/Al = 15) in the Ga/Al ratio range of 0.042 and 0.21. The decline in the TOF_{Ga} at Ga/Al ratios above 0.52 could also be rationalized by the replacement of Ga^+ – H^+ pair sites with less active Ga^+ – Ga^+ pair sites. The lack of proton pairs in the Al-lean Ga/H-ZSM-5 samples (Si/Al = 39) can only generate isolated Ga^+ sites from the lowest Ga/Al ratio tested. The decrease of TOF_{Ga} at Ga/Al ratios increase above 0.55 on these samples cannot be explained by the formation of Ga^+ – Ga^+ pair sites due to the lack of Ga^+ – H^+ pair sites to start with (Scheme 1b). One possible explanation is the formation of Ga oligomers as suggested by Bell and coworkers, [52] which are less active than isolated Ga^+ sites.

Apparent Activation Energy Measurements and Modeling

Activation energy measurements confirm that the apparent activation energy (E_{app}) of the PDH on the Ga⁺-H⁺ pair sites is lower than that on the isolated Ga⁺ sites. Apparent activation energies were determined based on the PDH rates on reduced Ga/H-ZSM-5 by varying the reaction temperature in the range of 530 – 570 °C. On H-ZSM-5 (Si/Al = 15), the E_{app} of the PDH was determined to be 188 kJ·mol⁻¹ (Figure 3a), a value consistent with the literature.^[47] The E_{app} decreases to 89.4 kJ·mol⁻¹ when Ga/Al ratio is increased to **Scheme 1.** Proposed structures of exchanged Ga species in Ga/H-ZSM-5 after reduction.



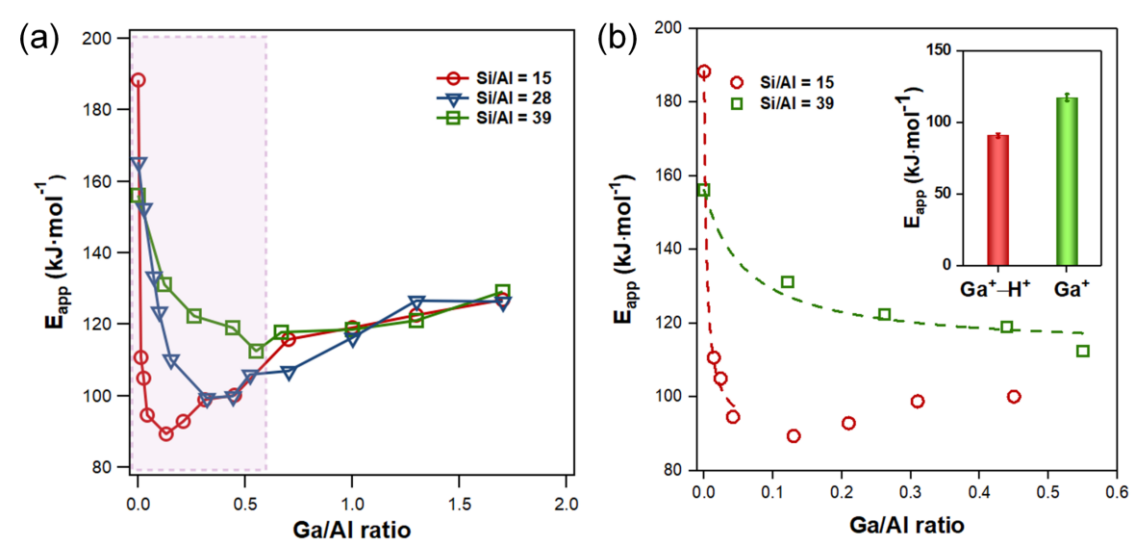


Figure 3. Apparent activation energy (E_{app}) of PDH on Ga/H-ZSM-5 as a function of Ga/Al ratios among different Si/Al ratios over the (a) entire, and (b) lower range of Ga/Al ratios (boxed region in (a)). Dotted lines in (b) represent the fitted E_{app} based on dual active sites models (details are provided in the Supporting Information). The inset in (b) shows the E_{app} of the Ga^+ -H⁺ pair sites and isolated Ga^+ sites in the PDH on samples with Si/Al ratios of 15 and 39, Ga/Al ratios from 0 - 0.042 and 0 - 0.55, respectively. The propane conversions are below 5.5% in the rate measurements.

0.13, showing that a small amount of Ga can effectively reduce the E_{app} . [46,47] This is consistent with the significantly enhanced PDH rate upon introducing Ga to H-ZSM-5 (Figure 1), as well as results reported by Bell and coworkers. [47] Further increase of the Ga/Al ratio up to 1.7 leads to a gradual increase of the E_{app} , indicating the formation of less active Ga species with the increase in the Ga loading (Scheme 1a). The E_{app} achieves a value of 127 kJ·mol⁻¹ at Ga/Al ratios of 1.7. A similar trend is observed for Ga/H-ZSM-5 with Si/Al ratios of 28. The E_{app} for Ga/H-ZSM-5(Si/Al=28) decreases from 166 to 110 kJ·mol⁻¹ as the Ga/Al ratio increases from 0 to 0.15, before rising again to 126 kJ·mol⁻¹ with further increase in the Ga/Al ratio (Figure 3a). On Ga/H-ZSM-5(Si/Al = 39), the measured E_{app} decreases from 156 to 113 kJ·mol⁻¹ as the Ga/Al ratio increases from 0 to 0.55, before gradually leveling off at 129 kJ·mol⁻¹ at a Ga/Al ratio of 1.7. The E_{app} on H-ZSM-5 (Si/Al = 39) is in agreement with the value reported by van Bokhoven and coworkers. [54] Also consistent with the literature, the E_{app} (156 kJ·mol⁻¹) of the BAS on H-ZSM-5 (Si/Al = 39) is lower than that on the Al-rich zeolite. [55] Three features of the dependence of the E_{app} on the Ga/Al ratio are worth noting

(Figure 3a): 1) the minimum E_{app} on Ga/H-ZSM-5 increases with the Si/Al ratio; 2) the minimum E_{app} occurs at an increasingly higher Ga/Al ratio as the Si/Al ratio rises; and 3) at the highest Ga/Al ratio tested (1.7), all tested catalyst exhibit nearly the same E_{app} regardless of Si/Al ratio. The initial decrease in the E_{app} as the Ga/Al ratio increases at low Ga loadings is attributed to the introduction of more active sites in the PDH than the BAS in H-ZSM-5, i.e., Ga⁺-H⁺ pair sites and isolated Ga⁺ sites. The observation that the value of the minimum E_{app} increases with the Si/Al ratio in the parent H-ZSM-5 indicates that the Ga-based active sites introduced are less active at higher Si/Al ratios. This interpretation agrees with the hypothesis that the more active Ga⁺-H⁺ pair sites are more abundant in Al-rich zeolites and the less active isolated Ga⁺ sites are more prevalent in samples with higher Si/Al ratios. The increasing Ga/Al ratio at which the minimum E_{app} is reached as the Si/Al ratio in the parent H-ZSM-5 increases could be rationalized by a similar line of reasoning as above. For Ga/H-ZSM-5(Si/Al = 15), the minimum E_{app} is expected to be on the catalyst with the highest density of the Ga⁺-H⁺ pair sites, which occurs at relatively low Ga/Al ratios (~0.05). Only isolated Ga⁺ sites are present on Ga/H-ZSM-5(Si/Al = 39) at low Ga loadings, which explains the slow reduction in the E_{app} with the Ga loading as BAS in the zeolite are gradually replaced by isolated Ga^+ sites. The E_{app} on Ga/H-ZSM-5 (Si/Al = 39) does not increase substantially at Ga/Al ratios above 0.5 (Figure 3a) because active sites for the PDH remain the isolated Ga⁺ sites, and the proposed Ga oligomers are reported to be inactive. [47] The E_{app} trend on Ga/H-ZSM-5 (Si/Al = 28) versus the Ga/Al ratio could be rationalized by the coexistence of BAS, Ga⁺-H⁺ pair sites and isolated Ga⁺ sites. The fact that the E_{app} at high Ga/Al ratios converge to a similar value suggests all samples are dominated by a similar type of Ga sites, e.g., Ga oligomers.

A simple dual-site model based on the reasoning above bas been constructed to more quantitatively understand the dependence of the E_{app} on the Ga/Al ratio. On Ga/H-ZSM-5 (Si/Al = 15) with Ga/Al ratios \leq

0.042, we assume that there are only two types of active sties in the PDH, i.e., BAS and Ga^+-H^+ pair sites, as proposed above.^[48] The E_{app} can be expressed as Eq. 5 below:

$$E_{app} = \frac{x_1 \cdot TOF_1 \cdot E_{a1} + x_2 \cdot TOF_2 \cdot E_{a2}}{x_1 \cdot TOF_1 + x_2 \cdot TOF_2}$$
 (5)

where x_1 and x_2 represent the ratio of remaining BAS to Al amount and Ga/Al ratio, respectively. The sum of x_1 and x_2 is the ratio of the BAS density to the Al density of the parent zeolite, which was determined in our recent work (Table S1).⁴⁸ The value of x_2 is an experimentally controlled variable, which is used to determine x_1 . TOF₁ and TOF₂ represent the measured BAS normalized and Ga normalized PDH rates, respectively (Figure 1). For Ga/H-ZSM-5 (Si/Al =15 and Ga/Al \leq 0.042), there are two types of active sites, i.e., BAS and Ga⁺-H⁺ pair sites. TOF_{Ga+-H+} is assumed to be equal to TOF_{Ga} (0.597 \pm 0.091 mol_{C3H8}·mol_{Ga}⁻¹·s·s⁻¹) based on the \sim 1:1 stoichiometry in the exchange between the BAS and Ga⁺ on these samples determined in our recent work.^[48] E_{a1} and E_{a2} represent the activation energy on the BAS and the Ga⁺-H⁺ pair sites respectively. Details of the model including derivations are described in the Supporting Information (Text S1 and Table S3). E_{a1} is experimentally determined to be 188 kJ·mol⁻¹ on H-ZSM-5 (Si/Al = 15), and the activation energy on Ga⁺-H⁺ pair sites (E_{a2}) could be obtained by fitting E_{app} at Ga/Al \leq 0.042 (Figure 3b), which is 90.8 \pm 1.5 kJ·mol⁻¹. This value is within the experimental errors identical to the lowest E_{app} determined on samples with a Si/Al ratio of 15 (89.4 kJ·mol⁻¹).

A similar strategy is applied to the PDH rates measured on Ga/H-ZSM-5 (Si/Al =39) to determine the activation of isolated Ga^+ sites in the PDH. Our previous work showed that exchanged gallium exists largely in the form of isolated Ga^+ sites in Ga/H-ZSM-5 (Si/Al =39).^[48] Thus, we assume there are two types of active sites in the PDH at $Ga/Al \le 0.55$: BAS and isolated Ga^+ sites. TOF_{Ga^+} is assumed to equal $TOF_{Ga}/60\%$ (0.075±0.008 mol_{C3H8}·mol_{Ga}-¹·s-¹) at Ga/Al ratios below 0.55 based on a ~ 0.6:1 stoichiometry in Ga exchange on these samples (~60% Ga atoms introduced exchanged with BAS to form Ga^+).^[48] Using the dual-site

model described above, the activation energy associated with isolated Ga⁺ sites is fitted to be 117±4.7 kJ·mol⁻¹ (Figure 3b and Table S3). The higher fitted activation energy for the isolated Ga⁺ sites than that of Ga⁺–H⁺ pair sites is consistent with the mechanism proposed in Scheme 1.

On Ga/H-ZSM-5 (Si/Al =28, Ga/Al \leq 0.52), a triple-site model is employed to fit the measured E_{app} , because BAS, Ga^+-H^+ pair sites and isolated Ga^+ sites co-exist at low Ga/Al ratios. The activation energies on all three types of sites on Ga/H-ZSM-5 (Si/Al =28) have been determined either by direct measurements (BAS, 166 kJ·mol⁻¹) or fitting using the dual-site model on Ga/H-ZSM-5 samples with low and high Si/Al ratios. The fraction of the exchanged Ga in the forms of Ga^+-H^+ pair sites and isolated Ga^+ sites can be

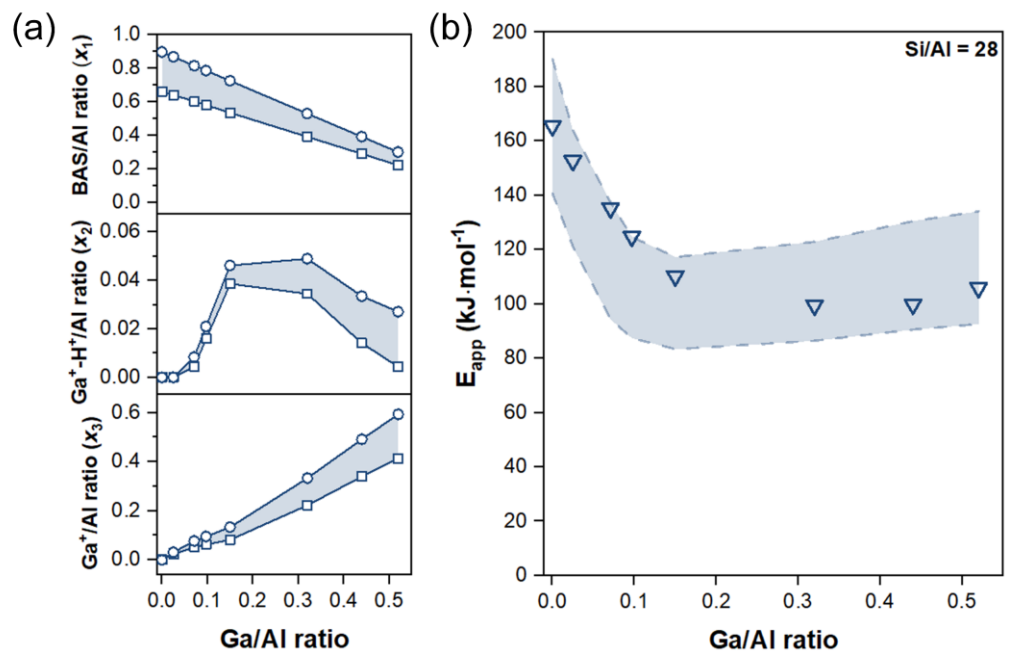


Figure 4. (a) Fitted fraction of different active species as a function of Ga/Al ratio on Ga/H-ZSM-5 with Si/Al ratio of 28 and Ga/Al ratios ranging from 0 to 0.52: x_1 , x_2 , x_3 represent the ratio of the remaining BAS, Ga⁺–H⁺ pair sites, isolated Ga⁺ sites to Al content, respectively. Shaded areas are estimated from experimental errors. (b) Apparent activation energy (E_{app}) of PDH on Ga/H-ZSM-5 (Si/Al = 28) as a function of Ga/Al ratios ranging from 0 to 0.52. Shaded area in (b) represent the simulated activation energy region based on triple-site models and experimental error bars (see Supporting Information for details). Reaction conditions: 530 – 570 °C, C₃H₈ partial pressure 5.07 kPa with balancing N₂. The propane conversion are below 5.5% in the rate measurements.

determined based on stoichiometry (Eqs. S6-S8, details are provided in Text S1). The fractions of three types of active sites at different Ga/Al ratios \leq 0.52 are plotted Figure 4a (data included in Table S4), with the BAS

 (x_1) and the isolated Ga^+ sites (x_3) decreasing and increasing monotonically, respectively. While the fraction of Ga^+ – H^+ pair sites (x_2) increases initially before dropping after Ga/Al > 0.2. The activation energy can be simulated with Eq. S9 (Text S1 and Table S4) by assuming a typical $\pm 15\%$ experimental uncertainty (Figure 4b, shaded area). All experimentally determined E_{app} values on Ga/H-ZSM-5 with a Si/Al of 28 ($Ga/Al \le 0.52$) are located in the shaded area, indicating the reliability of the estimated activation energies for Ga^+ – H^+ pair sites and isolated Ga^+ sites. This supports the three types of active sties identified in the PDH on Ga/H-ZSM-5. No attempt to extend the model to a fourth type of site, e.g., Ga^+ - Ga^+ or Ga oligomers, at higher Ga/Al ratios was made, because of the lack of independent determination of E_{app} for this type of site.

Interaction of GaH_x with Propane and Propylene

Since the first report of GaH_x species by Hensen and coworkers, [41] these species have been proposed to play a number of different roles in the PDH, e.g., reaction intermediate and active site. [43,46,47,50,56] However, experimental evidence regarding the interaction between GaH_x and propane and propylene has been scarce. [44] In-situ FTIR spectroscopy was employed to investigate the effect of C₃H₈ on GaH_x on Ga/H-ZSM-5 at reaction temperature. After reduction of Ga/H-ZSM-5 (Si/Al = 15, Ga/Al = 0.13) at 550 °C with H₂, IR bands attributable to Ga monohydride (2053 cm⁻¹) and Ga dihydride (2037 cm⁻¹) appear (Figure 5b(i)), as previously reported, [41,48,57] which were supported by DFT calculations by Bell and coworkers. [56] Upon introduction of C₃H₈ (0.27kPa) to the transmission cell at the same temperature, peaks attributable to gas phase C₃H₈ (2850 cm⁻¹ – 3000 cm⁻¹) are detected (Figure 5a (ii)), which agrees with bands detected in a control experiment (Figure S6). The GaH_x bands gradually diminish and largely disappear within 10 min (Figure 5b (vi)). The intensity of C₃H₈ bands also decreases over time (Figure 5a), indicating that C₃H₈ is gradually consumed in its dehydrogenation (the transmission cell is sealed after dosing C₃H₈, as in a batch reactor). Moreover, two peaks

centered at 3015 cm⁻¹ and 3055 cm⁻¹ appear and become more intense over time. These two peaks do not match those of gas phase of C_3H_8 or C_3H_6 (Figure S7), suggesting that they likely originate from reaction intermediates. Control experiment in which C_3H_6 (0.27 kPa) was introduced to a reduced Ga/H-ZSM-5 (Si/Al = 15 and Ga/Al = 0.13) at 550 °C showed the 3055 cm⁻¹ band with only weak bands corresponding to gas phase C_3H_6 (Figure S8a). In contrast, only gas phase C_3H_6 bands appeared when C_3H_6 was introduced to H-ZSM-5 (Si/Al = 15) at the same temperature (Figure S8b). These observations suggest that the 3055 cm⁻¹ band can be attributed to C_3H_6 adsorbed on Ga species. Thus, the gradual increase in the intensity of the 3055 cm⁻¹ band with time upon introduction of C_3H_8 indicates that C_3H_6 is produced via dehydrogenation on Ga/H-ZSM-5 (Figure 5a). The appearance of the 3015 cm⁻¹ band upon introduction of C_3H_8 to reduced Ga/H-ZSM-5 is likely to be attributed to the formation of reaction intermediates as this peak do not match those of gas phase C_3H_8 or C_3H_6 and is not observed upon the introduction of C_3H_6 to reduced Ga/H-ZSM-5 (Figures S6 and S7). Upon evacuation, the

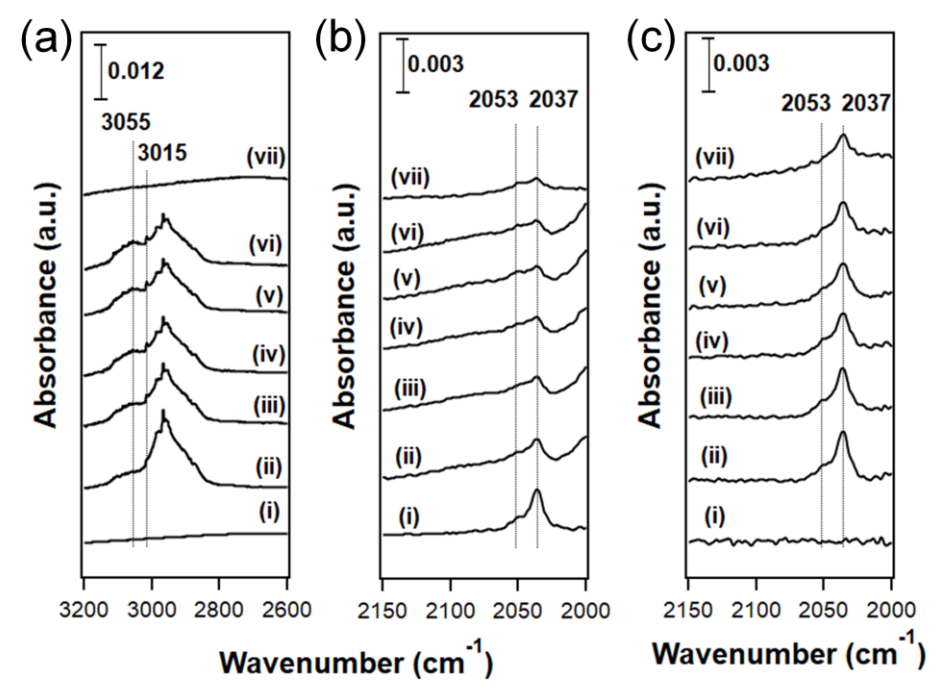


Figure 5. (a, b) FTIR spectra of C_3H_8 treatment on reduced Ga/H-ZSM-5 (Si/Al = 15, Ga/Al = 0.13): (i) before C_3H_8 treatment; (ii-vi) C_3H_8 treatment (0.27 kPa) for 2 min, 4 min, 6 min, 8 min, 10 min, respectively; (vii) after evacuation. (c) FTIR spectra of Ga/H-ZSM-5 (Si/Al = 15, Ga/Al = 0.13) (i) before H_2 treatment, (ii-vii) upon evacuating H_2 for 2 min, 4 min, 6 min, 8 min, 10 min and 30 min, respectively. Background spectrum is collected in the spectral cell with a dehydrated sample pellet at 550 °C under vacuum.

GaH_x bands do not change appreciably, but all hydrocarbon bands in the C-H stretching region disappear (Figure 5 (vii)), suggesting a weaker interaction with the catalyst surface than the hydride species. As expected, increasing the C₃H₈ pressure to 1.33 kPa leads to faster accumulation of bands corresponding to reaction intermediates and products (3015 cm⁻¹ and 3055 cm⁻¹), and less remaining GaH_x (Figure S9 (vii)). In contrast, the GaH_x bands largely remain unchanged after 10 min in vacuum, with the integrated peak area only decreasing by about 50% within 30 min (Figure 5c), showing that the presence of C₃H₈ significantly accelerates the decomposition of GaH_x. Similar observations were made on different Ga/Al ratios (Figures S9c and d, and S10). Control experiments rule out the possible influence of trace in the evacuated cell on the spectra based on the lack of the Ga(OH)_x band at ~3662 cm⁻¹ (Figure S11). The lack of GaH_x bands observed on Ga/Si-MFI and Ga/SiO₂ samples (Figure S12) suggests extraframework Ga species do not impact the spectral assignment in this work. Extraframework Ga species in Ga/H-ZSM-5, if present, are expected to resemble those on Ga/Si-MFI and Ga/SiO₂, and thus do not contribute to the GaH_x bands observed on Ga/H-ZSM-5. In addition, GaH_x bands on bulk Ga₂O₃ and Ga/Al₂O₃ appear at significantly lower wavenumbers (1996 cm⁻¹ and 1992 cm⁻¹ for GaH_x collected at 550 °C on bulk Ga₂O₃ and Ga/Al₂O₃, respectively, Figure S12). The lack of these lower wavenumber bands on Ga/H-ZSM-5 suggests that bulk Ga₂O₃ does not exist on reduced Ga/H-ZSM-5.

Propane promotion of the decomposition of GaH_x is also supported by kinetic measurements, in which the decomposition rate of GaH_x is determined via transmission FTIR spectroscopy. On Ga/H-ZSM-5 (Si/Al = 15 and Ga/Al = 0.042), the GaH_x consumption rate is determined by the fraction of decomposed GaH_x within 10 min under vacuum or 2 min in 0.27 kPa of C_3H_8 (or C_3H_6) in the temperature range of 530 - 570 °C. The apparent activation energies of GaH_x decomposition are 175 ± 16 , 150 ± 15 and 107 ± 9.9 kJ·mol⁻¹ under vacuum, in C_3H_8 and C_3H_6 , respectively (Figure 6a). We note that E_{app} is extracted by the Arrhenius equation, which only requires the knowledge relative, rather than absolute, decomposition rate of GaH_x . The reduction of E_{app} by 25

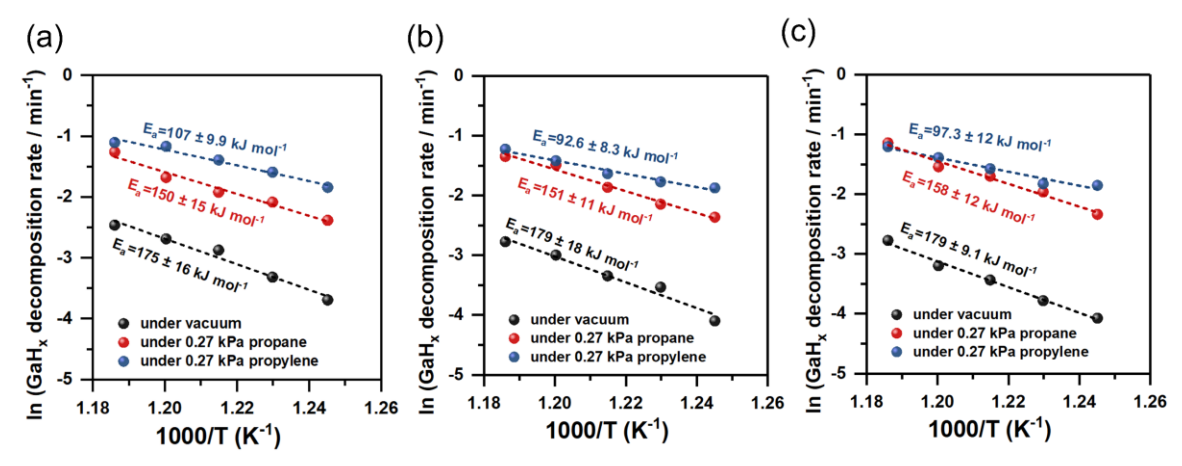


Figure 6. GaH_x consumption rate as a function of temperature over Ga/H-ZSM-5 (Si/Al = 15) with Ga/Al ratios of (a) 0.042, (b) 0.13 and (c) 0.31. The GaH_x decomposition rate is determined by % decomposed GaH_x during 10 min under vacuum or 2 min under 0.27 kPa propane or 2 min under 0.27 kPa propylene.

kJ·mol⁻¹ confirms that the presence of C_3H_8 promotes the decomposition of GaH_x . The lower E_{app} observed in cases in which C_3H_6 is present suggests that C_3H_6 is more effective in facilitating GaH_x decomposition. This is consistent with the observation of an IR band (3055 cm⁻¹) corresponding to adsorbed C_3H_6 on Ga sites (Figure 5a), without a corresponding band for adsorbed C_3H_8 . This could be rationalized by the stronger interaction between Ga sites and the C=C bond in C_3H_6 than the saturated bonds in C_3H_8 . The promotional effect of C_3H_8 on GaH_x decomposition indicates that C_3H_8 intimately interacts with the type of sites capable of forming GaH_x , i.e., Ga^+-H^+ pair sites. Similar GaH_x decomposition activation energies were determined in the same conditions on Ga/H-ZSM-5 (Si/Al = 15) with Ga/Al ratios of 0.13 and 0.31 (Figure 6b and c). This is consistent with the hypothesis that the GaH_x species observed via IR are only present on the Ga^+-H^+ pair sites at 550 °C, as only the density, rather than the structure, of the GaH_x species varies on Ga/H-ZSM-5 (Si/Al = 15) with different Ga-loadings.

Interaction of BAS with Propane and Propylene

FTIR spectroscopy shows that a fraction of BAS on Ga/H-ZSM-5 is consumed in the presence of C₃H₈ and C₃H₆. The band at 3591 cm⁻¹ assigned to BAS decreases in intensity upon introducing 0.27 kPa of C₃H₈ to Ga/H-ZSM-5 (Si/Al=15, Ga/Al=0.13) at 550 °C, which is clearly shown as a negative band in the spectra using a spectrum collected prior to propane dosage as the background (Figure 7a, original spectra are included in Figure S13). This is clear evidence of C₃H₈ interacting with BAS at the reaction temperature. The negative band disappears upon evacuation of propane, suggesting a dynamic, rather than irreversible, interaction between propane and BAS, e.g., formation of carbenium ion.^[59,60] A similar negative band is observed upon introducing C₃H₆ (Figure 7b), which can be similarly attributed to the BAS- C₃H₆ interaction. No decrease in the BAS band intensity is observed upon introduction of H₂ to the same Ga/H-ZSM-5 sample at 550 °C, confirming that the negative band stems from the interaction between hydrocarbons and BAS. A decrease of the BAS band intensity was also observed when C₃H₈ and C₃H₆ were introduced to H-ZSM-5 (Si/Al=15) at 550 °C (Figure 7c and d),

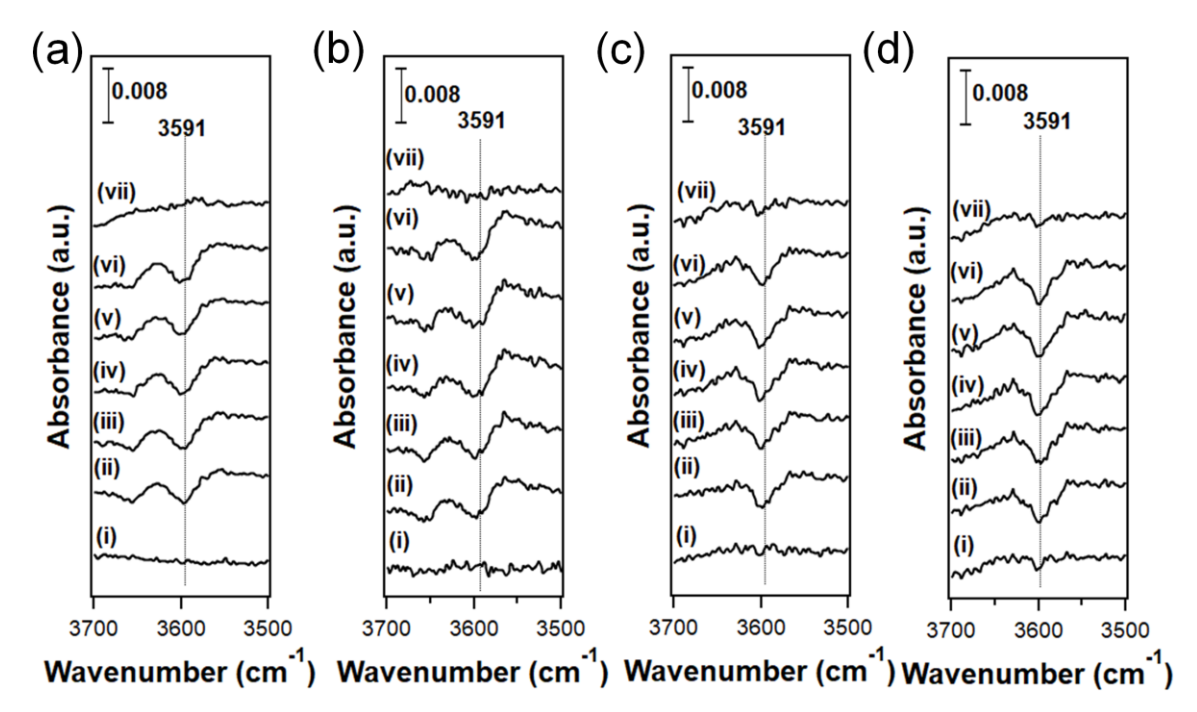


Figure 7. FTIR spectra of (a) C_3H_8 treatment and (b) C_3H_6 treatment on reduced Ga/H-ZSM-5 (Si/Al = 15, Ga/Al = 0.13), (c) C_3H_8 treatment and (d) C_3H_6 treatment on H-ZSM-5 (Si/Al = 15) at 550 °C: (i) before C_3H_8 or C_3H_6 treatment; (ii-vi) C_3H_8 or C_3H_6 treatment (0.27 kPa) for 2 min, 4 min, 6 min, 8 min, 10 min, respectively; (vii) after evacuation. Background spectrum is collected in the spectral cell with a reduced sample pellet at 550 °C under vacuum.

indicating the BAS-hydrocarbon interaction does not depend on the presence of Ga species. Similar observations were made on Ga/H-ZSM-5 and H-ZSM-5 samples with different Ga/Al ratios and hydrocarbon partial pressures (Figures S14-S18).

Propane Dehydrogenation Mechanism on Ga⁺–*H*⁺ *Pair Sites*

To date, proposed PDH mechanisms on Ga/H-ZSM-5 can be largely categorized into the alkyl mechanism and the carbenium mechanism. [35,36,46,47] The key difference between these mechanisms is the identity of sites on which C₃H₈ is activated: C₃H₈ is considered to be activated on Ga species to form a Ga alkyl intermediate in the alkyl mechanism, [46,47] while the carbenium mechanism argues that C₃H₈ is initially activated on the BAS to form a carbenium ion with Ga facilitating the recombination of H atom to form H₂. [35,36] The insitu FTIR spectroscopic results presented above show that propane interacts both with Ga species and BAS, which do not readily rule out either mechanism. However, detailed analysis suggests that the alkyl mechanism is more likely. If the primary function of Ga species in the PDH is to facilitate the evolution of H₂, then the E_{app} of the PDH is expected to be dominated by the decomposition of GaH_x. This is inconsistent with the higher E_{app} determined for GaH_x decomposition in the presence of propane than that of the PDH on Ga/H-ZSM-5 (~150 kJ·mol⁻¹ vs. ~90 kJ·mol⁻¹, as shown in Figures 6 and 3, respectively), indicating that the recombination of hydrogen atoms on GaH_x to form H₂ is not part of the PDH mechanism.

IR spectra of adsorbed intermediates provide further evidence supporting the alkyl mechanism. Due to the relatively weak interactions between hydrocarbons and the active sites of interest and high temperature, no detectable hydrocarbon intermediate is present upon evacuation of the propane treated Ga/H-ZSM-5 sample at 550 °C (Figure 5a). Introducing C₃H₈ to reduced Ga/H-ZSM-5 at high temperature and then cooling in the presence of C₃H₈ was employed as a strategy to preserve adsorbed reaction immediate for spectral detection at lower temperature (150 °C). On H-ZSM-5 (Si/Al=15), after exposure to C₃H₈ at 550 °C before quickly cooling

to 150 °C followed by evacuation, four peaks centered at 2976 cm⁻¹, 2937 cm⁻¹, 2903 cm⁻¹ and 2878 cm⁻¹ were present (Figure 8a(i)): these peaks have been assigned to antisymmetric CH₃, antisymmetric CH₂, symmetric CH₃ and symmetric CH₂ stretching modes, respectively. [61-63] These peaks could correspond to a reaction intermediate associated with BAS formed during the cooling process, which remains adsorbed at 150 °C after evacuation. On Ga/H-ZSM-5 samples (Si/Al=15, Ga/Al= 0.042 and 0.13), three peaks distinct from those on H-ZSM-5 centered at 2966 cm⁻¹, 2931 cm⁻¹ and 2874 cm⁻¹ were detected with similar procedures (Figure 8a(ii, iii)). These three new peaks have been assigned to antisymmetric CH₃, antisymmetric CH₂ and symmetric CH₂ stretching modes, respectively. [61-63] No hydrocarbon bands is present on H-ZSM-5 or Ga/H-ZSM-5 after evacuation when propane is introduced at 150 °C, indicating that these adsorbed hydrocarbons originate from C₃H₈'s interaction with catalytic sites at higher temperatures. This is in agreement with the Ga-methyl species detected by ¹³C solid-state NMR spectroscopy during CH₄ treatment on Ga/H-ZSM-5 at 300–550 °C. ^[64] The distinct C-H stretch bands on H-ZSM-5 and Ga/H-ZSM-5 show that different adsorbed intermediates are present on these two catalysts.

The relative intensity of the GaH and GaH₂ infrared bands provide additional mechanistic insights. As expected, no GaH_x band is present on H-ZSM-5 (Figure 8b(i)), while both GaH and GaH₂ bands appear at 150 °C on Ga/H-ZSM-5 (Figure 8b(ii, iii), black traces). The GaH band is the more intense feature on the C₃H₈ treated sample, while the GaH₂ band is more prominent on H₂ treated Ga/H-ZSM-5 at 150 °C (Figure 8b(ii, iii), red traces). It could be inferred that the hydrocarbon intermediate is more effective in displacing/consuming GaH₂ than GaH. The lack of the Ga(OH)_x band at ~3672 cm⁻¹ at 150 °C confirms the negligible impact of any trace amount of water in the evacuated cell on these spectra (Figure S19). Heating leads to the desorption of the adsorbed hydrocarbon species on Ga/H-ZSM-5 (Si/Al = 15, Ga/Al = 0.13) from 150 °C to 350 °C, while the

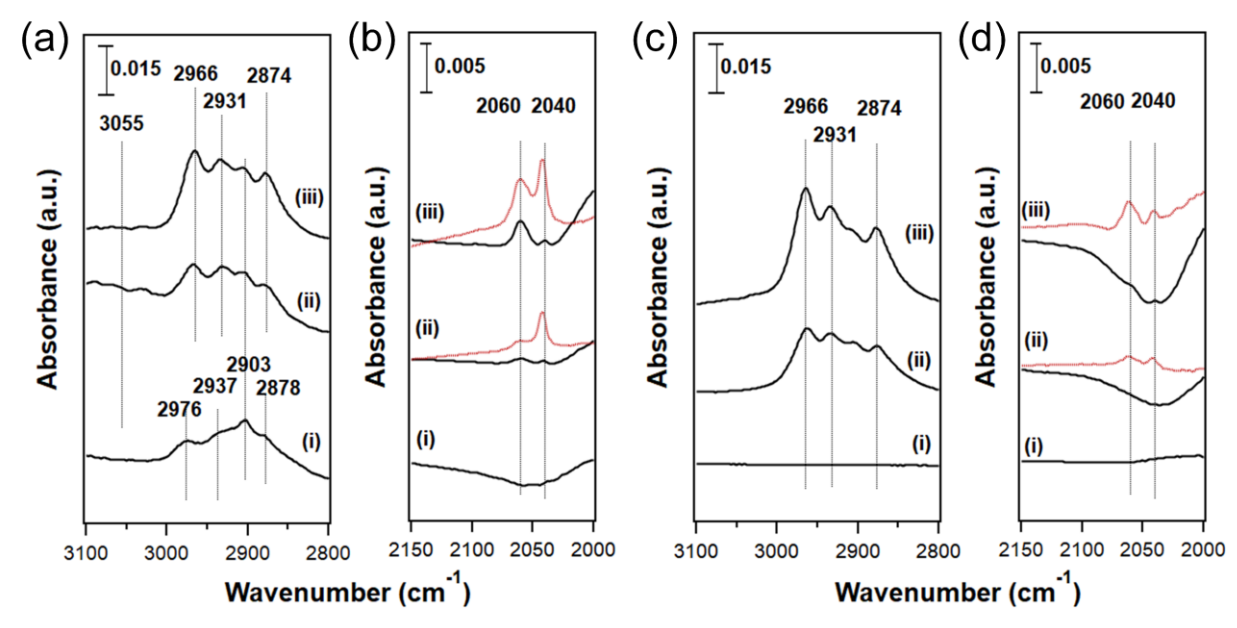


Figure 8. FTIR spectra of C_3H_8 treatment on (a, b) Ga/H-ZSM-5 (Si/Al = 15) with Ga/Al ratios of (i) 0, (ii) 0.042, (iii) 0.13 and (c, d) Ga/H-ZSM-5 (Si/Al = 39) with Ga/Al ratios of (i) 0, (ii) 0.12, (iii) 0.44. Black and red traces represent spectra on the reduced Ga/H-ZSM-5 cooled down from 550 °C to 150 °C under 1.33 kPa C_3H_8 , followed by evacuating the cell and under vacuum, respectively. Background spectrum is collected in the spectral cell with a sample pellet dehydrated at 550 °C and cooled down to 150 °C under vacuum.

 GaH_x bands remain until 500 °C (Figure S20). This is consistent with the observation of a $[Ga^{3+}(H^-)(C_2H_5^-)]^+$ species by Hensen and coworkers when heating reduced Ga/H-ZSM-5 in the presence of ethane to 250 °C^[42]. Similar observations were made on H-ZSM-5 and Ga/H-ZSM-5 with a Si/Al ratio of 39 (Figure 8c and d). The lack of C-H stretching bands on H-ZSM-5 could be attributed to the low Al density in this sample.

A number of mechanistic deductions can be made based on the spectral results (Scheme 2). C₃H₈ can be activated at BAS, isolated Ga⁺ sites and Ga⁺–H⁺ pair sites, though the resulting intermediates are different on BAS and Ga species. We hypothesize that carbenium ions are formed on the BAS as proposed by Iglesia and coworkers (Scheme 2a)^[36,60], and alkyl species are formed on Ga species (Scheme 2b and c). The fact that the C-H stretching modes on Ga/H-ZSM-5 with primarily Ga⁺–H⁺ pair sites (Si/Al=15, Ga/Al=0.13) and isolated Ga⁺ sites (Si/Al=39, Ga/Al=0.44) are almost identical (Figure 8a and c) suggests that Ga⁺, regardless of its isolation or pairing with a neighboring proton, is the site activating C₃H₈. The neighboring H⁺ in the Ga⁺–H⁺

pair sites is proposed to facilitate the abstraction of the hydride in the propyl group, leading to the formation of C₃H₆, H₂, and a [GaH]²⁺ species balanced by two neighboring framework negative charges. This hypothesis is supported by two observations: 1) the GaH species is preferentially preserved or less consumed when exposing GaH_x containing catalysts to C₃H₈ at 550 °C (Figures 5b and 8b); and 2) the E_{app} of the PDH reaction on Ga/H-ZSM-5 is lower than that of the GaH_x decomposition. Since GaH₂ is the dominant hydride species on reduced Ga/H-ZSM-5, the measured E_{app} in the GaH_x decomposition should be representative of the decomposition of GaH₂. It follows that the decomposition of GaH₂ is not part of the PDH mechanism, otherwise the GaH₂ decomposition is expected to be the rate limiting step (RLS) of the mechanism and the measured E_{app} of the PDH should be equal to that of the RLS. This mechanism agrees with two recently proposed mechanisms by Schreiber et al. [46] and Phadke et al. [47] in recognizing the importance of the proximity between Ga⁺ and H⁺ sites in the PDH. Instead of considering [GaH]²⁺ as the active site in the PDH reaction, [47] we propose that [GaH]²⁺ is merely an intermediate formed in the rate-limiting hydride extraction of the propyl group (Step 2, Scheme 2c). This is supported by the observation that the GaH band at 2053 cm⁻¹ is less impacted upon introducing C₃H₈ to the reduced Ga/H-ZSM-5 (Si/Al=15, Ga/Al=0.13) at 550 °C (Figure 5b), as active sites for C₃H₈ activation are expected to interact with C₃H₈ and thereby lose their infrared signature. The interaction between C₃H₈ and GaH_x is reflected in the accelerated rates and lowered activation energy of GaH_x decomposition in the presence of C₃H₈. This analysis is further corroborated by the coexistence of the adsorbed alkyl species and the GaH band when the catalyst is cooled to 150 °C in the presence of propane (Figure 8b). Our mechanism bears more resemblance to the one proposed by Schreiber et al. largely based on computations, [46] with the key difference being whether the hydrogen evolution occurs prior to or concurrently with the hydride abstraction of the adsorbed propyl group. Our rationale for the latter is based on the observation of the GaH band in the presence

Scheme 2. Schematic of proposed mechanisms for the PDH on (a) H⁺, (b) isolated Ga⁺ and (c) Ga⁺-H⁺.

(a)
$$+ C_{3}H_{8} \longrightarrow H_{3}C CH_{3} H_{2} \longrightarrow H_{2} \longrightarrow H_{3}C CH_{3} H_{4}C CH_{3} H_{5}C CH_{3} H_{5}C CH_{5}CH_{5}C CH_{5}C CH_{$$

of the C₃H₈, which does not appear in the stepwise mechanism. We note that the proposed mechanism is also compatible with the earlier isotopic labeling results by Iglesia and coworkers,^[36,60] which indicated multiple fast C-H activations in C₃H₈ prior to the RLS in the PDH. When a mixture of C₃H₈ and C₃D₈ is introduced to Ga/H-ZSM-5, H/D scrambling is expected to occur on BAS, either with or without a neighboring Ga⁺, leading to a mixture of C₃H_xD_{8-x}. The dehydrogenation of this mixture then is expected to lead to a corresponding isotopic mixture of C₃H_yD_{6-y}, as observed by Biscardi et al.^[36,60]

Conclusions

In summary, PDH rates on Ga/H-ZSM-5 with varying Si/Al ratios (15, 28 and 39) and Ga/Al ratio (0 –

1.7) were measured, demonstrating that catalytic activity is sensitive to both Si/Al and Ga/Al ratios. Intrinsic

PDH activity of two Ga species, Ga⁺-H⁺ pair and isolated Ga⁺ sites, were determined, with the former being

more active by a factor of ~15. Activity energy measurements and modeling provided further evidence

supporting the superior activity of the Ga+-H+ pair sites, and determined the activation energy for each type of

species in the PDH. Activation energy of the decomposition of GaH_x is lower by ~25 kJ mol⁻¹ in the presence

of C₃H₈ than under vacuum, indicating the effective interaction between C₃H₈ and Ga⁺-H⁺ pair sites. Moreover,

the activation energy of GaH_x decomposition is higher than that of the PDH, indicating that the hydrogen

evolution from GaH_x decomposition is not part of the PDH mechanism. Together with additional in-situ FTIR

spectroscopic evidence, C₃H₈ is proposed to be activated on Ga⁺-H⁺ pair and isolated Ga⁺ sites, followed by

hydride elimination and the concurrent formation of C₃H₆ and H₂. GaH is proposed to be a reaction intermediate

in the PDH, while GaH₂ does not participate in the reaction.

AUTHOR INFORMATION

Corresponding Author

*E-mail: b xu@pku.edu.cn

ASSOCIATED CONTENT

Supporting Information

The Supporting Information is available free of charge on the ACS Publications website at DOI:

ACKNOWLEDGMENT

26

We acknowledge the support by the RAPID manufacturing institute, USA, supported by the Department of Energy (DOE) Advanced Manufacturing Office (AMO), award number DE-EE0007888-6.5. Y.Y. also acknowledges the support of the US National Science Foundation under the grant number of CBET-1803246.

References

- (1) Sattler, J. J. H. B.; Ruiz-Martinez, J.; Santillan-Jimenez, E.; Weckhuysen, B. M. Catalytic Dehydrogenation of Light Alkanes on Metals and Metal Oxides. *Chem. Rev.* **2014**, *114*, 10613–10653.
- (2) Bhan, A.; Delgass, W. N. Propane Aromatization over HZSM-5 and Ga/HZSM-5 Catalysts. *Catal. Rev. Sci. Eng.* **2008**, *50*, 19–151.
- (3) Zacharopoulou, V.; Lemonidou, A. Olefins from Biomass Intermediates: A Review. Catalysts 2018, 8, 2.
- (4) Al-Douri, A.; Sengupta, D.; El-Halwagi, M. M. Shale Gas Monetization A Review of Downstream Processing to Chemicals and Fuels. *J. Nat. Gas Sci. Eng.* **2017**, *45*, 436–455.
- (5) James, O. O.; Mandal, S.; Alele, N.; Chowdhury, B.; Maity, S. Lower Alkanes Dehydrogenation: Strategies and Reaction Routes to Corresponding Alkenes. *Fuel Process. Technol.* **2016**, *149*, 239–255.
- (6) Bruijninex, P. C. A.; Weckhuysen, B. M. Shale Gas Revolution: An Opportunity for the Production of Biobased Chemicals? *Angew. Chem. Int. Ed.* **2013**, *52*, 11980–11987.
- (7) Hu, Z.-P.; Yang, D.; Wang, Z.; Yuan, Z.-Y. State-of-the-Art Catalysts for Direct Dehydrogenation of Propane to Propylene. *Chin. J. Catal.* **2019**, *40*, 1233–1254.
- (8) He, Y.; Song, Y.; Laursen, S. The Origin of the Special Surface and Catalytic Chemistry of Ga-Rich Ni₃Ga in the Direct Dehydrogenation of Ethane. *ACS Catal.* **2019**, *9*, 10464–10468.
- (9) Bauer, T.; Maisel, S.; Blaumeiser, D.; Vecchietti, J.; Taccardi, N.; Wasserscheid, P.; Bonivardi, A.; Görling, A.; Libuda, J. Operando DRIFTS and DFT Study of Propane Dehydrogenation over Solid- and Liquid-

Supported Ga_xPt_y Catalysts. ACS Catal. 2019, 9, 2842–2853.

- (10) Raman, N.; Maisel, S.; Grabau, M.; Taccardi, N.; Debuschewitz, J.; Wolf, M.; Wittkämper, H.; Bauer, T.; Wu, M.; Haumann, M.; Papp, C.; Görling, A.; Spiecker, E.; Libuda, J.; Steinrück, H.; Wasserscheid, P. Highly Effective Propane Dehydrogenation Using Ga—Rh Supported Catalytically Active Liquid Metal Solutions. *ACS Catal.* **2019**, *9*, 9499–9507.
- (11) He, Y.; Song, Y.; Cullen, D. A.; Laursen, S. Selective and Stable Non-Noble-Metal Intermetallic Compound Catalyst for the Direct Dehydrogenation of Propane to Propylene. *J. Am. Chem. Soc.* **2018**, *140*, 14010–14014.
- (12) Searles, K.; Chan, K. W.; Mendes Burak, J. A.; Zemlyanov, D.; Safonova, O.; Copéret, C. Highly Productive Propane Dehydrogenation Catalyst Using Silica-Supported Ga-Pt Nanoparticles Generated from Single-Sites. *J. Am. Chem. Soc.* **2018**, *140*, 11674–11679.
- (13) Raad, M.; Astafan, A.; Hamieh, S.; Toufaily, J.; Hamieh, T.; Comparot, J. D.; Canaff, C.; Daou, T. J.; Patarin, J.; Pinard, L. Catalytic Properties of Ga-Containing MFI-type Zeolite in Cyclohexane Dehydrogenation and Propane Aromatization. *J. Catal.* **2018**, *365*, 376–390.
- (14) Searles, K.; Siddiqi, G.; Safonova, O. V.; Copéret, C. Silica-Supported Isolated Gallium Sites as Highly Active, Selective and Stable Propane Dehydrogenation Catalysts. *Chem. Sci.* **2017**, *8*, 2661–2666.
- (15) Kim, W.; So, J.; Choi, S.; Liu, Y.; Dixit, R. S.; Sievers, C.; Sholl, D. S.; Nair, S.; Jones, C. W. Hierarchical Ga-MFI Catalysts for Propane Dehydrogenation. *Chem. Mater.* **2017**, *29*, 7213–7222.
- (16) Sattler, J. J. H. B.; Gonzalez-Jimenez, I. D.; Luo, L.; Stears, B. A.; Malek, A.; Barton, D. G.; Kilos, B. A.; Kaminsky, M. P.; Verhoeven, T. W. G. M.; Koers, E. J.; Baldus, M.; Weckhuysen, B. M. Platinum-Promoted Ga/Al₂O₃ as Highly Active, Selective, and Stable Catalyst for the Dehydrogenation of Propane. *Angew. Chem. Int. Ed.* **2014**, *53*, 9251–9256.

- (17) Zhao, Z.; Wu, T.; Xiong, C.; Sun, G.; Mu, R.; Zeng, L.; Gong, J. Hydroxyl-Mediated Non-oxidative Propane Dehydrogenation over VO_x/γ-Al₂O₃ Catalysts with Improved Stability. *Angew. Chem. Int. Ed.* **2018**, 57, 6791–6795.
- (18) Xie, Y.; Luo, R.; Sun, G.; Chen, S.; Zhao, Z.; Mu, R.; Gong, J. Facilitating the Reduction of V–O Bonds on VO_x/ZrO₂ Catalysts for Non-Oxidative Propane Dehydrogenation. *Chem. Sci.* **2020**, *11*, 3845–3851.
- (19) Kong, N.; Fan, X.; Liu, F.; Wang, L.; Lin, H.; Li, Y.; Lee, S. Single Vanadium Atoms Anchored on Graphitic Carbon Nitride as a High-Performance Catalyst for Non-oxidative Propane Dehydrogenation. *ACS Nano* **2020**, 14, 5772–5779.
- (20) Gu, Y.; Liu, H.; Yang, M.; Ma, Z.; Zhao, L.; Xing, W.; Wu, P.; Liu, X.; Mintova, S.; Bai, P.; Yan, Z. Highly Stable Phosphine Modified VO_x/Al₂O₃ Catalyst in Propane Dehydrogenation. *Appl. Catal. B* **2020**, *274*, 119089.
- (21) Schweitzer, N. M.; Hu, B.; Das, U.; Kim, H.; Greeley, J.; Curtiss, L. A.; Stair, P. C.; Miller, J. T.; Hock, A. S. Propylene Hydrogenation and Propane Dehydrogenation by a Single-Site Zn²⁺ on Silica Catalyst. *ACS Catal.* **2014**, *4*, 1091–1098.
- (22) Almutairi, S. M. T.; Mezari, B.; Magusin, P. C. M. M.; Pidko, E. A.; Hensen, E. J. M. Structure and Reactivity of Zn-Modified ZSM-5 Zeolites: The Importance of Clustered Cationic Zn Complexes. *ACS Catal.* **2012**, *2*, 71–83.
- (23) Chen, C.; Zhang, S.; Wang, Z.; Yuan, Z.-Y. Ultrasmall Co Confined in the Silanols of Dealuminated Beta Zeolite: A Highly Active and Selective Catalyst for Direct Dehydrogenation of Propane to Propylene. *J. Catal.* **2020**, *383*, 77–87.
- (24) Dai, Y.; Gu, J.; Tian, S.; Wu, Y.; Chen, J.; Li, F.; Du, Y.; Peng, L.; Ding, W.; Yang, Y. γ-Al₂O₃ Sheet-Stabilized Isolate Co²⁺ for Catalytic Propane Dehydrogenation. *J. Catal.* **2020**, *381*, 482–492.

- (25) Moselage, M.; Li, J.; Ackermann, L. Cobalt-Catalyzed C-H Activation. ACS Catal. 2016, 6, 498-525.
- (26) Tan, S.; Hu, B.; Kim, W.; Pang, S. H.; Moore, J. S.; Liu, Y.; Dixit, R. S.; Pendergast, J. G.; Sholl, D. S.; Nair, S.; Jones, C. W. Propane Dehydrogenation over Alumina-Supported Iron/Phosphorus Catalysts: Structural

Evolution of Iron Species Leading to High Activity and Propylene Selectivity. ACS Catal. 2016, 6, 5673–5683.

- (27) Yun, J. H.; Lobo, R. F. Catalytic Dehydrogenation of Propane over Iron-Silicate Zeolites. *J. Catal.* **2014**, 312, 263–270.
- (28) Yun, J. H.; Lobo, R. F. Radical Cation Intermediates in Propane Dehydrogenation and Propene Hydrogenation over H-[Fe] Zeolites. *J. Phys. Chem. C* **2014**, *118*, 27292–27300.
- (29) Maeno, Z.; Yasumura, S.; Wu, X.; Huang, M.; Liu, C.; Toyao, T.; Shimizu, K. Isolated Indium Hydrides in CHA Zeolites: Speciation and Catalysis for Nonoxidative Dehydrogenation of Ethane. *J. Am. Chem. Soc.* **2020**, *142*, 4820–4832.
- (30) Zhang, Y.; Zhao, Y.; Otroshchenko, T.; Lund, H.; Pohl, M.; Rodemerck, U.; Linke, D.; Jiao, H.; Jiang, G.; Kondratenko, E. V. Control of Coordinatively Unsaturated Zr sites in ZrO₂ for Efficient C–H Bond Activation. *Nat. Commun.* **2018**, *9*, 3794.
- (31) Otroshchenko, T.; Kondratenko, V. A.; Rodemerck, U.; Linke, D.; Kondratenko, E. V. ZrO₂-Based Unconventional Catalysts for Non-Oxidative Propane Dehydrogenation: Factors Determining Catalytic Activity. *J. Catal.* **2017**, *348*, 282–290.
- (32) Otroshchenko, T.; Sokolov, S.; Stoyanova, M.; Kondratenko, V. A.; Rodemerck, U.; Linke, D.; Kondratenko, E. V. ZrO₂-Based Alternatives to Conventional Propane Dehydrogenation Catalysts: Active Sites, Design, and Performance. *Angew. Chem. Int. Ed.* **2015**, *54*, 15880–15883.
- (33) Hu, Z.-P.; Chen, C.; Ren, J.-T.; Yuan, Z.-Y. Direct Dehydrogenation of Propane to Propylene on Surface-Oxidized Multiwall Carbon Nanotubes. *Appl. Catal. A* **2018**, *559*, 85–93.

- (34) Hu, Z.-P.; Zhao, H.; Chen, C.; Yuan, Z.-Y. Castanea Mollissima Shell-Derived Porous Carbons as Metal-Free Catalysts for Highly Efficient Dehydrogenation of Propane to Propylene. *Catal. Today* **2018**, *316*, 214–222. (35) Iglesia, E.; Baumgartner, J. E.; Price, G. L. Kinetic Coupling and Hydrogen Surface Fugacities in Heterogeneous Catalysis: I. Alkane Reactions on Te/NaX, H-ZSM5, and Ga/H-ZSM5. *J. Catal.* **1992**, *134*, 549–571.
- (36) Biscardi, J. A.; Iglesia, E. Structure and Function of Metal Cations in Light Alkane Reactions Catalyzed by Modified H-ZSM5. *Catal. Today* **1996**, *31*, 207–231.
- (37) Yu, S. Y.; Yu, G. J.; Li, W.; Iglesia, E. Kinetics and Reaction Pathways for Propane Dehydrogenation and Aromatization on Co/H-ZSM5 and H-ZSM5. *J. Phys. Chem. B* **2002**, *106*, 4714–4720.
- (38) Li, W.; Yu, S. Y.; Meitzner, G. D.; Iglesia, E. Structure and Properties of Cobalt-Exchanged H-ZSM5 Catalysts for Dehydrogenation and Dehydrocyclization of Alkanes. *J. Phys. Chem. B* **2001**, *105*, 1176–1184.
- (39) Biscardi, J. A.; Meitzner, G. D.; Iglesia, E. Structure and Density of Active Zn Species in Zn/H-ZSM5 Propane Aromatization Catalysts. *J. Catal.* **1998**, *179*, 192–202.
- (40) García-Sanchez, M.; Magusin, P. C. M. M.; Hensen, E. J. M.; Thüne, P. C.; Rozanska, X.; van Santen, R. A. Characterization of Ga/HZSM-5 and Ga/HMOR Synthesized by Chemical Vapor Deposition of Trimethylgallium. *J. Catal.* **2003**, *219*, 352–361.
- (41) Kazansky, V. B.; Subbotina, I. R.; van Santen, R. A.; Hensen, E. J. M. DRIFTS Study of the Chemical State of Modifying Gallium Ions in Reduced Ga/ZSM-5 Prepared by Impregnation I. Observation of Gallium Hydrides and Application of CO Adsorption as A Molecular Probe for Reduced Gallium Ions. *J. Catal.* **2004**, 227, 263–269.
- (42) Kazansky, V. B.; Subbotina, I. R.; van Santen, R. A.; Hensen, E. DRIFTS Study of the Nature and Chemical Reactivity of Gallium Ions in Ga/ZSM-5 II. Oxidation of Reduced Ga Species in ZSM-5 by Nitrous

- Oxide or Water. J. Catal. 2005, 233, 351-358.
- (43) Kazansky, V. B.; Subbotina, I. R.; Rane, N.; van Santen, R. A.; Hensen, E. J. M. On Two Alternative Mechanisms of Ethane Activation over ZSM-5 Zeolite Modified by Zn²⁺ and Ga¹⁺ Cations. *Phys. Chem. Chem. Phys.* **2005**, *7*, 3088–3092.
- (44) Rodrigues, V. D.; Faro Júnior, A. C. On Catalyst Activation and Reaction Mechanisms in Propane Aromatization on Ga/HZSM5 Catalysts. *Appl. Catal. A* **2012**, *435–436*, 68–77.
- (45) Rodrigues, V. D.; Vasconcellos, F. J.; Faro Júnior, A. D. C. Mechanistic Studies through H–D Exchange Reactions: Propane Aromatization in HZSM5 and Ga/HZSM5 Catalysts. *J. Catal.* **2016**, *344*, 252–262.
- (46) Schreiber, M. W.; Plaisance, C. P.; Baumgärtl, M.; Reuter, K.; Jentys, A.; Bermejo-Deval, R.; Lercher, J. A. Lewis-Brønsted Acid Pairs in Ga/H-ZSM-5 To Catalyze Dehydrogenation of Light Alkanes. *J. Am. Chem. Soc.* **2018**, *140*, 4849–4859.
- (47) Phadke, N. M.; Mansoor, E.; Bondil, M.; Head-Gordon, M.; Bell, A. T. Mechanism and Kinetics of Propane Dehydrogenation and Cracking over Ga/H-MFI Prepared via Vapor-Phase Exchange of H-MFI with GaCl₃. *J. Am. Chem. Soc.* **2019**, *141*, 1614–1627.
- (48) Yuan, Y.; Brady, C.; Annamalai, L.; Lobo, R. F.; Xu, B. Ga Speciation in Ga/H-ZSM-5 by In-situ Transmission FTIR Spectroscopy. *J. Catal.* **2021**, 393, 60–69.
- (49) Cho, H. J.; Kim, D.; Li, J.; Su, D.; Xu, B. Zeolite-Encapsulated Pt Nanoparticles for Tandem Catalysis. *J. Am. Chem. Soc.* **2018**, *140*, 13514–13520.
- (50) Rane, N.; Overweg, A. R.; Kazansky, V. B.; van Santen, R. A.; Hensen, E. Characterization and Reactivity of Ga⁺ and GaO⁺ Cations in Zeolite ZSM-5. *J. Catal.* **2006**, *239*, 478–485.
- (51) Xu, B.; Li, T.; Zheng, B.; Hua, W.; Yue, Y.; Gao, Z. Enhanced Stability of HZSM-5 Supported Ga₂O₃ Catalyst in Propane Dehydrogenation by Dealumination. *Catal. Lett.* **2007**, *119*, 283–288.

- (52) Phadke, N. M.; Van der Mynsbrugge, J.; Mansoor, E.; Getsoian, A. B.; Head-Gordon, M.; Bell, A. T. Characterization of Isolated Ga³⁺ Cations in Ga/H-MFI Prepared by Vapor-Phase Exchange of H-MFI Zeolite with GaCl₃. *ACS Catal.* **2018**, *8*, 6106–6126.
- (53) Song, C.; Chu, Y.; Wang, M.; Shi, H.; Zhao, L.; Guo, X.; Yang, W.; Shen, J.; Xue, N.; Peng, L.; Ding, W. Cooperativity of Adjacent Brønsted Acid Sites in MFI Zeolite Channel Leads to Enhanced Polarization and Cracking of Alkanes. *J. Catal.* **2017**, *349*, 163–174.
- (54) Xu, B.; Sievers, C.; Hong, S.; Prins, R.; van Bokhoven, J. Catalytic Activity of Brønsted Acid Sites in Zeolites: Intrinsic Activity, Rate-Limiting Step, and Influence of the Local Structure of the Acid Sites. *J. Catal.* **2006**, *244*, 163–168.
- (55) Janda, A.; Bell, A. T. Effects of Si/Al Ratio on the Distribution of Framework Al and on the Rates of Alkane Monomolecular Cracking and Dehydrogenation in H-MFI. *J. Am. Chem. Soc.* **2013**, *135*, 19193–19207. (56) Mansoor, E.; Head-Gordon, M.; Bell, A. T. Computational Modeling of the Nature and Role of Ga Species for Light Alkane Dehydrogenation Catalyzed by Ga/H-MFI. *ACS Catal.* **2018**, *8*, 6146–6162.
- (57) Serykh, A. I.; Kolesnikov, S. P. On the Nature of Gallium Species in Gallium-Modified Mordenite and MFI Zeolites. A Comparative DRIFT Study of Carbon Monoxide Adsorption and Hydrogen Dissociation. *Phys. Chem. Chem. Phys.* **2011**, *13*, 6892.
- (58) Sen, A. Catalytic Functionalization of Carbon-Hydrogen and Carbon-Carbon Bonds in Protic Media. *Acc. Chem. Res.* **1998**, *31*, 550–557.
- (59) Biscardi, J. A.; Iglesia, E. Reaction Pathways and Rate-Determining Steps in Reactions of Alkanes on H-ZSM5 and Zn/H-ZSM5 Catalysts. *J. Catal.* **1999**, *182*, 117–128.
- (60) Biscardi, J. A.; Iglesia, E. Isotopic Tracer Studies of Propane Reactions on H–ZSM5 Zeolite. *J. Phys. Chem. B* **1998**, *102*, 9284–9289.

- (61) Rebrov, E. V.; Simakov, A. V.; Sazonova, N. N.; Stoyanov, E. S. Dinitrogen Formation over Low-Exchanged Cu-ZSM-5 in the Selective Reduction of NO by Propane. *Catal. Lett.* **1999**, *58*, 107–118.
- (62) Solymosi, F.; Németh, R.; Óvári, L.; Egri, L. Reactions of Propane on Supported Mo₂C Catalysts. *J. Catal.* **2000**, *195*, 316–325.
- (63) Yu, P.; Damiran, D. Heat-Induced Changes to Lipid Molecular Structure in Vimy Flaxseed: Spectral Intensity and Molecular Clustering. *Spectrochimica Acta Part A* **2011**, *79*, 51–59.
- (64) Luzgin, M. V.; Gabrienko, A. A.; Rogov, V. A.; Toktarev, A. V.; Parmon, V. N.; Stepanov, A. G. The "Alkyl" and "Carbenium" Pathways of Methane Activation on Ga-Modified Zeolite BEA: ¹³C Solid-State NMR and GC-MS Study of Methane Aromatization in the Presence of Higher Alkane. *J. Phys. Chem. C* **2010**, *114*, 21555–21561.